AD_____

Award Number: DAMD17-03-1-0014

TITLE: FGF Signaling and Dietary Factors in the Prostate

PRINCIPAL INVESTIGATOR: Fen Wang, Ph.D.

CONTRACTING ORGANIZATION: Texas A&M University
                            College Station, Texas   77843

REPORT DATE: March 2005

TYPE OF REPORT: Annual

PREPARED FOR: U.S. Army Medical Research and Materiel Command
                Fort Detrick, Maryland   21702-5012

DISTRIBUTION STATEMENT: Approved for Public Release;
                        Distribution Unlimited

The views, opinions and/or findings contained in this report are
those of the author(s) and should not be construed as an official
Department of the Army position, policy or decision unless so
designated by other documentation.

20050826 047

REPORT DOCUMENTATION PAGE

1. AGENCY USE ONLY (Leave blank)	2. REPORT DATE March 2005	3. REPORT TYPE AND DATES COVERED Annual (1 Mar 2004 – 28 Feb 2005)

4. TITLE AND SUBTITLE
FGF Signaling and Dietary Factors in the Prostate

5. FUNDING NUMBERS
DAMD17-03-1-0014

6. AUTHOR(S)
Fen Wang, Ph.D.

7. PERFORMING ORGANIZATION NAME(S) AND ADDRESS(ES)
Texas A&M University
College Station, Texas 77843

E-Mail: fwang@IBT.tmc.edu

8. PERFORMING ORGANIZATION REPORT NUMBER

9. SPONSORING / MONITORING AGENCY NAME(S) AND ADDRESS(ES)
U.S. Army Medical Research and Materiel Command
Fort Detrick, Maryland 21702-5012

10. SPONSORING / MONITORING AGENCY REPORT NUMBER

11. SUPPLEMENTARY NOTES

12a. DISTRIBUTION / AVAILABILITY STATEMENT
Approved for Public Release; Distribution Unlimited

12b. DISTRIBUTION CODE

13. ABSTRACT (Maximum 200 Words)

Purpose: To study the FGF signaling axis in prostate homeostasis and tumorigenesis, to evaluate dietary factors in modulating FGF signals in the prostate.

Scope: To develop mouse models resembling human prostate tumor progressions for screening therapeutic strategies for prostate cancers and evaluating dietary factors in prostate cancer prevention.

Major Finding: Ectopic expression of the constitutively-active FGFR1 (caFGFR1) in the prostate induces high-grade prostatic intraepithelial neoplasia (PIN) in transgenic mice in an expression level-dependent manner. Repression of the resident FGFR2 in the prostate also disturbs homeostasis in the prostate as well as potentiated the PIN lesions induced by the ectopic caFGFR1.

Up-to-date Progress: Establishing mouse colonies with prostate-specific disruption of *Fgfr2* loci and expression of the ectopic caFGFR1 in dependent of androgen for further characterizations of the FGF signaling and dietary factors in prostate lesions. Generation of a conditional expression vector for expressing FGFR1 in the prostate. Characterization of the prostate of FGFR2 conditional null mice.

Significance: Together with previous data from the Dunning prostate tumor model, the findings demonstrate that aberrant FGF signals in the prostate strongly disrupt tissue homeostasis, and promote prostate tumor development and progression. The model provides a useful tool for evaluating other tumor initiating factors, including those that cause genetic instability and other oncogenic lesions in prostate tumorigenesis.

14. SUBJECT TERMS
Growth factors, tyrosine kinase, mouse model, transgenic mouse, nutrition, tumor prevention tissue specific gene inactivation

15. NUMBER OF PAGES
20

16. PRICE CODE

17. SECURITY CLASSIFICATION OF REPORT	18. SECURITY CLASSIFICATION OF THIS PAGE	19. SECURITY CLASSIFICATION OF ABSTRACT	20. LIMITATION OF ABSTRACT
Unclassified	Unclassified	Unclassified	Unlimited

TABLE OF CONTENTS

INTRODUCTION

The prostate consists of epithelium and stromal compartments separated by a basement membrane. The communications and mutual regulations between the two compartments are critical for growth, develop, and function of the prostate. The fibroblast growth factor (FGF) signaling complex has long been implicated in mediating these regulatory communications, which consists of 22 single polypeptide ligands, 4 transmembrane tyrosine kinase receptors (FGFR), and a pool of highly heterogenic heparan sulfate proteoglycans (HSPG) in the extracellular matrix. Appearances of the FGF signaling complexes are highly temporally and spatially specific; aberrant expression is often correlated with prostate cancer progression in human and experimental animal models. We previously demonstrated that ectopic expression of a constitutively active FGFR1 mutant (caFGFR1) in the prostate epithelium induces age- and expression level-dependent prostatic intraepithelial neoplasia (PIN). Furthermore, depression of FGFR2 signaling in the prostate also disturbs homeostasis in the prostate and induces prostate hyperplasia. The project is to study whether FGFR1 and FGFR2 elicit receptor-specific activity in the prostate, to determine whether ectopic expression of FGFR1 and depression of FGFR2 synergistically induce prostatic lesion, and to evaluate dietary factors in modulating FGF signals in the prostate. The long-term goal is to develop mouse models resembling human prostate tumor progressions for screening therapeutic strategies for prostate cancers and evaluating dietary factors in prostate cancer prevention.

BODY

Task 1. Characterization of the prostate of caFGFR1/KDNR bigenic mice.

      a. *Generation of enough male caFGFR1/KDNR bigenic mice for the study by crossing caFGFR1 and KDNR transgenic mice.*

      b. *Collecting prostate tissue of bigenic and control mice at different ages, performing serial section of the prostate and characterization of prostate tissue structures.*

Progress:

To date, the prostates of the ARR2PBi-caFGFR1/KDNR bigenic mice and the parental transgenic strains have been phenotypically characterized, and the main results are published in Cancer Research (1). The outlines of the main findings are as follows; please refer to the attachments for the details.

i. ARR2PBi-caFGFR1 mice developed high grade PIN within 8 months.

In general, exposure to the ectopic FGFR1 kinase induces PIN in the caFGFR1 transgenic mice; the development and severity of the PIN lesion is expression level- and time-dependent. The phenotype includes increase in prostate tissue mass, increase in mitosis in the prostate, and disorganized and atypical luminal epithelial cells in prostate lumens. Furthermore, the expression of cytokeratins is significantly reduced in epithelial foci with high-grade PIN lesions, especially those with cribriform structures. The high-grade PIN foci, particularly those with cribriform structures, often have a disrupted stromal layer indicated by discontinuous and faint staining of smooth muscle cell characteristic α-actin. Frequently, the over proliferating epithelial cells disrupt the basement membrane, invade the stromal compartment, and form small epithelial foci in the space between the basement membrane and stromal cells. This indicates that the epithelial cells in these foci are not just pushed through the stromal layer and form glandule-like structures. Instead, these epithelial cells form microinvasion foci in the stromal compartment, which are more advanced lesions than high grade PIN.

ii. Cooperation between ectopic expression of FGFR1 and depression of FGFR2 signaling in perturbation of prostate homeostasis.

Depression of the endogenous FGFR2 signaling alone by expression of a kinase inactive mutant (KDNR) only induces low grade PIN lesions in the prostate. Yet, it synergistically perturbs prostate tissue homeostasis with the ectopic FGFR1 kinase in the prostate of caFGFR1/KDNR bigenic mice. Depression of the endogenous FGFR2 signaling significantly increases the neuroendocrine cell population in the prostate of the caFGFR1 transgenic mice. Furthermore, depression of the FGFR2 signaling in the prostate of the PB-caFGFR1 transgenic mice potentiates PIN lesion development, and shortens the dormant period before developing PIN lesions, which expresses caFGFR1 kinase at low levels.

Task 2. Generation of ROSA-caFGFR1/Fgfr2c/c mice, and characterization of the prostates.

a. *Construction of the ROSA-caFGFR1 knock-in vector.*

b. *Introduction of the ROSA-caFGFR1 construct to mouse embryo stem cells.*

c. *Generation of founders bearing the ROSA-caFGFR1 locus.*

d. *Establishing colonies from each positive founder and verifying gemline integration of the ROSA-caFGFR1 locus.*

e. *Collecting prostates from ROSA-caFGFR1/Fgfr2$^{c/c}$ and control mice, performing serial section of the prostate and characterization of the prostate tissue structures.*

f. *Access the impact of dietary factors on the initiation and development of prostate lesions in ROSA-caFGFR1/Fgfr2$^{c/c}$ mice.*

Progress:

i. Generation of the ROSA-caFGFR1 knock-in mice.

The ROSA26 locus encodes an unessential gene that is strongly and ubiquitously expressed, which is ideal for tissue specific expression of a target gene together with the Cre-loxP recombination technology. To knock-in the conditionally expressed caFGFR1 transgene, a ROSA-caFGFR1 knock-in vector was constructed (Fig. 1). Since the caFGFR1 cDNA is inserted downstream of the neo cassette, which has multiple translational stop sites and polyA additions sites, the caFGFR1 cDNA will not be transcribed until the loxP flanked neo cassette is removed by Cre recombinase.
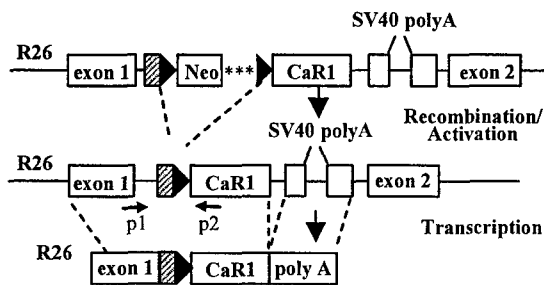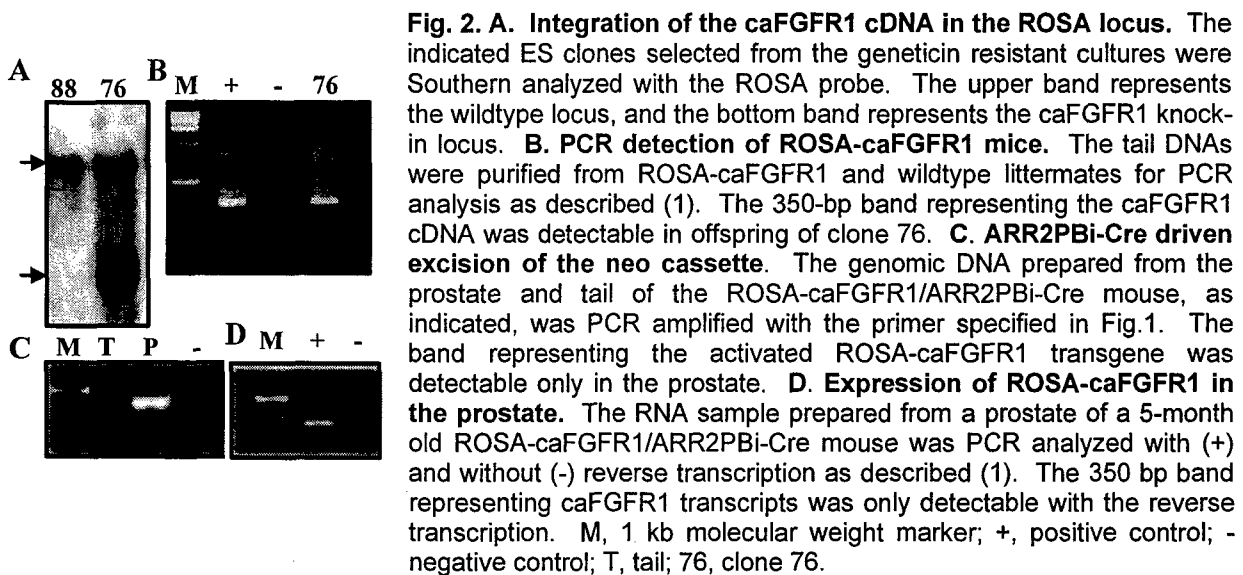

Fig. 1. Scheme for generation of ROSA-caFGFR1 mice. The expression of caFGFR1 is blocked by the loxP flanked neo cassette without the Cre recombinase. Removal of the neo cassette mediated by Cre recombinase activates the transcription of FGFR1 cDNA. After splicing, the matured transcript only encodes caFGFR1. p1 and p2 are the diagnostic primers for detection of the excision of the neo cassette; triangles, loxP sites; hatch box, splice acceptor sequence; neo, neo cassette; *, translational stop codon; caFGFR1, caFGFR1 cDNA; polyA, the splice site and the polyA addition site of SV40 T antigens; exon1, 3, exon1, 3 of the ROSA26 locus.

The ROSA-caFGFR1 DNA was excised from the vector and introduced to AK7 mouse embryo stem (ES) cells by electroporation. Five colonies were identified to have correct recombination. Among them, A76 was selected for the microinjection. Four chimera founders were generated from the injection, and one founder has gemline integration, as demonstrated with the PCR screen of caFGFR1 in the agouti offspring followed by conformation with Southern analysis (Fig. 2A,B). To determine whether the ROSA-caFGFR1 transgene could be activated by Cre recombinase mediated excision of the neo cassette and to assess the expression profile of the caFGFR1, the ROSA-caFGFR1 mouse was crossed with the ARR2PBi-Cre transgenic mouse that expressed the Cre recombinase in prostate epithelial cells (4). Prostate tissues of 5-month old ROSA-caFGFR1/ARR2PBi-Cre bigenic mice were collected for genomic and RNA preparations. PCR analyses with the primers indicated in Fig. 1 show that the neo cassette is excised specifically in prostate, but not tail, DNA (Fig. 2C). To assess whether the ROSA-caFGFR1 transgene is expressed in the prostate, RNA samples from the prostate of 5-month old bigenic mice were analyzed with Northern blotting with a probe specific for human FGFR1, which does not hybridize with the endogenous mouse FGFR1 transcript. The results show in Fig. 2D show that expression of the caFGFR1 transgene is lower than the detection limit, although RT-PCR analyses revealed that the caFGFR1 is expressed in the prostate.

Fig. 2. A. Integration of the caFGFR1 cDNA in the ROSA locus. The indicated ES clones selected from the geneticin resistant cultures were Southern analyzed with the ROSA probe. The upper band represents the wildtype locus, and the bottom band represents the caFGFR1 knock-in locus. **B. PCR detection of ROSA-caFGFR1 mice.** The tail DNAs were purified from ROSA-caFGFR1 and wildtype littermates for PCR analysis as described (1). The 350-bp band representing the caFGFR1 cDNA was detectable in offspring of clone 76. **C. ARR2PBi-Cre driven excision of the neo cassette.** The genomic DNA prepared from the prostate and tail of the ROSA-caFGFR1/ARR2PBi-Cre mouse, as indicated, was PCR amplified with the primer specified in Fig.1. The band representing the activated ROSA-caFGFR1 transgene was detectable only in the prostate. **D. Expression of ROSA-caFGFR1 in the prostate.** The RNA sample prepared from a prostate of a 5-month old ROSA-caFGFR1/ARR2PBi-Cre mouse was PCR analyzed with (+) and without (-) reverse transcription as described (1). The 350 bp band representing caFGFR1 transcripts was only detectable with the reverse transcription. M, 1 kb molecular weight marker; +, positive control; - negative control; T, tail; 76, clone 76.

ii. Generation of ROSA-caFGFR1$_{v2}$ knock-in mice.

The most likely reason that the ROSA-caFGFR1 transgene has a low transcription activity is that the transgene has an intron sequence downstream of the stop codon of the caFGFR1 cDNA. According to the nonsense-mediated decay theory, the mRNA is not stable if the stop codon is not in the last exon. To correct this problem, second generation of the ROSA-caFGFR1 transgene was generated (Fig. 3) in which the intronic sequence in the SV40 non coding region was removed. The ROSA-caFGFR1 fragment was excised from the vector and was introduced to AK7 mouse embryo stem (ES) cells by electroporation. The transfected AK7 cells were selectively grown in the presence of geneticin. About four hundred geneticin resistant clones were selected for Southern analyses with the ROSA probe. Six colonies were identified to have the correct recombination. Among them, H12 and G4 were selected for microinjections. The microinjected blastcysts were transferred to a pseudopregnant foster mother for full term development. Two high percentage chimeric founders were generated from the injections. Currently, we are testing whether the founder has gemline integration.
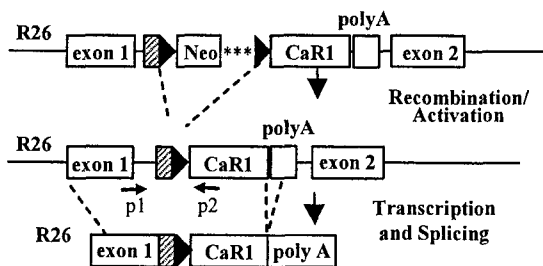

Fig. 3. The ROSA-caFGFR1$_{v2}$ knock-in vector. The intronic sequence of the sv-40 3'-end non-coding region was removed from the original vector sequence shown in Fig. 1. An sv-40 polyA additional site was directly ligated downstream of the stop codon of FGFR1 cDNA to prevent degradation of the transcript due to the nonsense mediated decay. p1 and p2 are the diagnostic primers for detection of the excision of the neo cassette; triangles, loxP sites; hatch box, splice acceptor sequence; neo, neo cassette; *, translational stop codon; caFGFR1, caFGFR1 cDNA; polyA, the splice site and the polyA addition site of SV40 T antigens; exon1, 3, exon1, 3 of the ROSA26 locus

7

iii. Generation of transgenic mice with conditional expression of FGFR1.

Generating genetically engineered mice that express high levels of the constitutively active caFGFR1 in the prostate epithelial cells independent of androgen regulation and differentiation is important to the project. Therefore, we adopted an alternative way to generate mice with conditional expression of caFGFR1 transgene. A conditional expression vector was constructed as illustrated in Fig. 4. *In vitro* transfection to COS-7 cells showed that the expression of the vector is Cre recombinase dependent (Fig. 4b). The cDNA encoding caFGFR1 has been inserted to the vector, and the transgene will be used for pronuclear injection to generate transgenic mice. The positive founders will be crossed with the ARR2PBi-Cre mice for activation of the caFGFR1 transgene in the prostate, and the expression level of the transgene will be determined in the prostate with and without coexpression of the Cre recombinase.
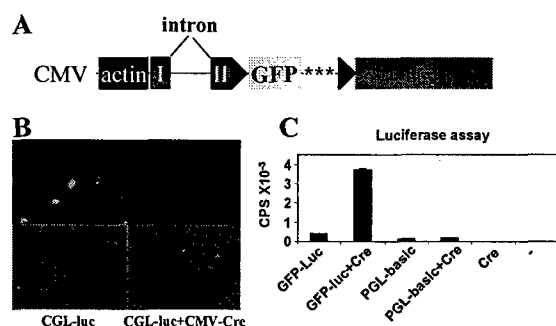

Fig. 4. A. Schematic of the luciferase conditional expression (LUC-CE) vector. The expression of luciferase driven by the chicken CMV/actin enhancer-promoter is blocked by the floxed GFP cassette. Cre mediated-removal of the GFP cassette activates the expression. **B and C. Conditional expression of GFP (B) or luciferase (C).** The cos-7 cells were transfected with the Luc-CE vector with or without coexpression with the CMV-Cre plasmid as indicated. **B.** Upper panel, the light output of the GFP was observed with a fluorescence microscope; lower panel, light microscopy of the same cells in the upper panels. **C.** The luciferase activities in transfected cos-7 cells were analyzed with the luciferase assay kit and quantitated with a scintillation counter as described (3). I and II, exons 1 and 2 sequences of the chick β-actin gens, *, polyA additional signal, triangles, loxP elements.

iv. Characterization of the prostates with disrupted resident FGFR2 signaling axis in epithelial cells.

To disrupt the resident FGFR2 in the epithelium of the prostate, the mice with loxP flanked FGFR2 allele were crossed with the ARR2PBi-Cre transgenic mice. Prostate tissues from 5-month old FGFR2-floxed and FGFR2 conditional-null mice were harvested for RNA preparations. Results in Fig. 5 showed that the expression of FGFR2 was significantly reduced in the prostate. Preliminary results showed that the disrupted FGFR2 null prostates were significantly larger than the FGFR2 floxed littermates. The average wet weight of the FGFR2 null prostate was 283 mg, which is about 2.5 times larger than that of FGFR2 floxed littermates (Fig. 5). Histochemistry analyses revealed that the FGFR2-null prostate developed high-grade PIN at the age of 12 months or older. Moreover, the expression of cytokeratin 18 that is highly expressed in well-differentiated prostate epithelial cells was significantly reduced in FGFR2 null prostates. On the other hand, the expression of cytokeratin 14 that is expressed in less-

differentiated prostate basal cells was increased in FGFR2 null prostate. This suggests that disruption of the resident FGFR2 perturbs tissue homeostasis in the prostate. Detailed histological characterizations are undertaken currently.
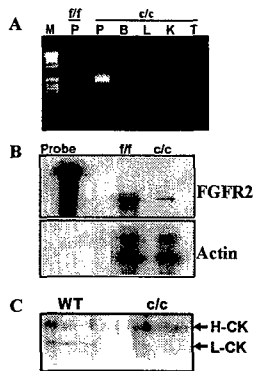

Fig. 5. *A. Prostate-specific disruption of FGFR2.* Genomic DNAs from the prostate and indicated tissues from FGFR2 conditional null and floxed mice were extracted, and the 500 bp fragment representing the null allele of FGFR2 was PCR amplified for as described (2). *B. Reduction of FGFR2 expression in Fgfr2$^{c/c}$ prostate.* Total RNAs were extracted from the prostates of indicated mice. The expression of FGFR2 was assessed by the RNase protection assays with probes for FGFR2 (top panel), or β-actin for loading controls (bottom panel). *C. Disruption of FGFR2 changes cytokeratin expression in the prostate.* The prostate of FGFR2 condition null mice and wildtype littermates were harvested at the age of 1 year and homogenized in 1% Triton-PBS. The lysates equivalent to 20 μg proteins were separated on SDS-PAGE, and cytokeratins were detected with anti-pan cytokeratin antibodies. M, 1 kb DNA marker; P, prostate; B, bladder; L, liver; K, kidney; T, testis; f/f, Fgfr2$^{f/f}$; c/c, Fgfr2$^{c/c}$; H-CK and L-CK, high molecular weight and low molecular weight cytokeratin, respectively.

v. To evaluate dietary effects on prostate lesions induced by disruption of the resident FGFR2 signaling.

The ROSA-caFGFR1 knock-in mice have not been fully characterized to date, therefore, it is too early to test the dietary effect on tissue homeostasis in the prostate of ROSA-caFGFR1/FGFR2 null mice. Instead, since the FGFR2 null/ARR2PBi-caFGFR1 prostate has been characterized, we are carrying out the experiments with the FGFR2 condition null mice with or without expression of the caFGFR1 transgene in the prostate. Twenty each of newly weaned mice of FGFR2 condition null and FGFR2 floxed mice were set aside and fed with high fat/cholesterol (40% calories from saturated fat, 2% cholesterol) diet and regular diet. The mice will be sacrificed at the ages of 8, 10, 12, 14, and 16 months. The prostate tissue will be collected and histologically examined, including tissue structures, immunohistochemistry analysis with anti-cytokeratin, and α-actin antibodies. The expression of the resident FGFR2 will also be accessed. In addition, another group of mice will be set up and fed a caloric restriction diet (50% calories) soon to determine whether restriction of calories has impact on PIN lesions in the FGFR2 null prostate.

KEY RESEARCH ACCOMPLISHMENTS

1. Establish a highly efficient prostate specific Cre mouse model for tissue specific disruption and activation of genes in the prostate. The Cre recombinase efficiently excises the loxP-flanked fragment in the FGFR2 locus in the prostate as well as in ROSA-caFGFR1 knock-in mice for conditional expression of the constitutively active FGFR1 (caFGFR1) in the prostate.

2. Characterize the phenotype of the ARR2PBi-caFGFR1 transgenic mice that express caFGFR1 at high levels. The mice develop high-grade prostatic intraepithelial neoplasia (PIN) within one year. The initiation and progression of PIN is caFGFR1 expression level dependent.

3. Characterize the phenotype of the PB-caFGFR1/KDNR and ARR2PBi-caFGFR1/KDNR bigenic mice. Suppression of the resident FGFR2 signaling and expression of the caFGFR1 synergistically disrupt homeostasis and induce PIN lesions in the prostate.

4. Generation of a line of ROSA-caFGFR1 knock-in mice that carry a silent caFGFR1 coding sequence in the ROSA locus for conditional expression of the caFGFR1 in target tissues. The neo cassette that suppresses expression of the caFGFR1 could be removed in the prostate via Cre-mediated recombination.

5. Generation of a colony of mice with prostate-specific disruption of FGFR2. The average wet weight of FGFR2-null prostate tissues were at least two times larger that that of the FGFR2-floxed mice and had an increased population of basal epithelial cells. The histology characterization of the FGFR2-null prostate is undertaken currently.

6. Construction of a conditional expression transgenic vector for conditional expression of FGFR1. In vitro results showed that the vector had a low background expression of luciferase with a silencing GFP cassette; excision of the GFP cassette activated the luciferase expression. Currently, we are in the process of cloning the caFGFR1 cDNA into the vector for generation of the transgenic mice.

7. Construction and generation of ROSA-caFGFR1v2 knock-in mice. The knock-in vector was constructed; five clones of mouse embryonic stem cells with the predicted recombination were generated. Two clones were injected so far. Two chimeric males were generated. A breeding colony will be setup as soon as the mice are mature.

REPORTABLE OUTCOMES

1. Publications:

a. Jin, C., K. McKeehan, and F. Wang (2003) Transgenic mouse with high Cre recombinase activity in all prostate lobes, seminal vesicle, and ductus deferens. *The Prostate* **57**:160-164.

b. Jin, C., K. McKeehan, W. Guo, S. Jauma, M. M. Ittmann, B. Foster, N. M. Greenberg, W. L. McKeehan, and F. Wang (2003) Cooperation between ectopic FGFR1 and depression of FGFR2 signaling in induction of prostatic intraepithelial neoplasia in mouse prostate *Cancer Res.* **63**: 8784-8790.

c. Zhang, Y., Y. Lin, C. Bowles, and F. Wang (2004). Direct cell cycle regulation by the fibroblast growth factor receptor (FGFR) kinase through phosphorylation-dependent release of Cks1 from FGFR substrate 2. *J. Biol. Chem.* **279**: 55348-55354.

2. Abstract:

1. Kerstin McKeehan, Scot Jauma, and Fen Wang (2004) Aberrant FGF signaling axis disrupts homeostasis and induces prostatic intraepithelial neoplasia in the prostate of genetically altered mice. *AACR Annual Meeting Abstract*

2. Fen Wang. (2004) The fibroblast growth factor signaling axis and polysaccharides of the extracellular matrix in neuron regeneration. The Third Symposium on Neuroscience for Young Scholars Worldwide, Guangzhou, China

3. Presentations:

a. **The FGF signaling axis in prostate homeostasis and tumorigenesis.** Annual meeting of the Society of Chinese Bioscientists America, Texas Chapter. Houston, TX (2003).

b. **The FGF signaling axis in prostate homeostasis and tumorigenesis.** Sealy Center for Cancer Cell Biology, University of Texas, Medical Branch. Galveston, TX (2003).

c. **The FGF signaling axis in prostate homeostasis and tumorigenesis.** Department of Molecular and Cellular Biology, Baylor College of Medicine, Houston, TX (2003)

d. **The FGF signaling in the prostate: from molecules to mice.** Meharry Medical College-Vanderbilt University Alliance. Nashville, TN (2004).

e. **The extracellular matrix and the FGF signaling in spinal cord regeneration.** The Spinal Cord Injury Workshop sponsored by The Institute of Rehabilitation and Research (TIRR) in Galveston. (2004).

f. **The FGF signaling in the prostate: from molecules to mice.** The Life Science College, Xiamen University. Xiamen, China. (2004).

g. **Establishing genetically engineered mouse model for cancer research.** The Biotechnology College, Jimei University. Xiamen, China (2004).

h. **The fibroblast growth factor signaling axis and polysaccharides of the extracellular matrix in neuron regeneration.** The Third Symposium on Neuroscience for Young Scholars Worldwide, Guangzhou, China (2004)

4. Requests for mouse models through collaborations:

15

CONCLUSIONS

The prostatic intraepithelial neoplasia (PIN) development and homeostasis perturbation in the prostate of caFGFR1 transgenic mice are caFGFR1 expression level dependent. Repression of the FGFR2 signaling potentiated perturbation of prostate homeostasis induced by the ectopic caFGFR1 kinase. The results further suggest that aberrant FGF signaling in the prostate is a strong factor in disruption of tissue homeostasis, and is a strong promoter for prostate tumor development and progression. In addition, the ARR2PBi-caFGFR1/KDNR mouse model provides a useful tool for evaluating other tumor initiating factors, including genetic instability and other oncogenic lesions in prostate tumorigenesis.

REFERENCES

1. Jin, C., McKeehan, K., Guo, W., Jauma, S., Ittmann, M. M., Foster, B., Greenberg, N. M., McKeehan, W. L., and Wang, F. (2003) Cooperation between ectopic FGFR1 and depression of FGFR2 in induction of prostatic intraepithelial neoplasia in the mouse prostate. *Cancer Res* **63**, 8784-8790

2. Yu, K., Xu, J., Liu, Z., Sosic, D., Shao, J., Olson, E. N., Towler, D. A., and Ornitz, D. M. (2003) Conditional inactivation of FGF receptor 2 reveals an essential role for FGF signaling in the regulation of osteoblast function and bone growth. *Development* **130**, 3063-3074

3. Wang, F., McKeehan, K., Yu, C., and McKeehan, W. L. (2002) Fibroblast growth factor receptor 1 phosphotyrosine 766: molecular target for prevention of progression of prostate tumors to malignancy. *Cancer Res* **62**, 1898-1903

4. Jin, C., McKeehan, K., and Wang, F. (2003) Transgenic mouse with high Cre recombinase activity in all prostate lobes, seminal vesicle, and ductus deferens. *Prostate* **57**, 160-164

APPENDICES LIST:

1. Zhang, Y., Y. Lin, C. Bowles, and F. Wang (2004). Direct cell cycle regulation by the fibroblast growth factor receptor (FGFR) kinase through phosphorylation-dependent release of Cks1 from FGFR substrate 2. *J. Biol. Chem.* **279**: 55348-55354.

Direct Cell Cycle Regulation by the Fibroblast Growth Factor Receptor (FGFR) Kinase through Phosphorylation-dependent Release of Cks1 from FGFR Substrate 2*⑤

Yongyou Zhang, Yongshun Lin, Courtney Bowles, and Fen Wang‡

From the Center for Cancer Biology and Nutrition, Institute of Biosciences and Technology, Texas A & M University System Health Science Center, Houston, Texas 77030-3303

Fibroblast growth factors (FGFs) are upstream activators of the mitogen-activated protein kinase pathway and mitogens in a wide variety of cells. However, whether the mitogen-activated protein kinase pathway solely accounts for the induction of cell cycle or anti-apoptotic activity of the FGF receptor (FGFR) tyrosine kinase is not clear. Here we report that cell cycle inducer Cks1, which triggers ubiquitination and degradation of $p27^{Kip1}$, associates with the unphosphorylated form of FGFR substrate 2 (FRS2), an adaptor protein that is phosphorylated by FGFR kinases and recruits downstream signaling molecules. FGF-dependent activation of FGFR tyrosine kinases induces FRS2 phosphorylation, causes release of Cks1 from FRS2, and promotes degradation of $p27^{Kip1}$ in 3T3 cells. Since degradation of $p27^{Kip1}$ is a key regulatory step in activation of the cyclin E/A-Cdk complex during the G_1/S transition of the cell cycle, the results suggest a novel mitogenic pathway whereby FGF and other growth factors that activate FRS2 directly activate cyclin-dependent kinases.

The fibroblast growth factor $(FGF)^1$ family is a ubiquitously expressed transmembrane signaling family that elicits receptor-mediated regulatory effects on cell growth, function, differentiation, and death. The FGF ligands are single polypeptides consisting of 22 genetically distinct homologues, and the FGF receptors (FGFRs) are transmembrane tyrosine kinases encoded by four homologous gene products, which complex with pericellular matrix heparan sulfates independent of the FGF ligand (1, 2). Binding of FGF ligands to FGFR-heparan sulfate complexes activates the kinase activity and transmits regulatory signals to downstream signaling mediators or targets. Accumulating reports demonstrate that FGFRs elicit diverse regulatory activities that are cell type- and FGFR-specific as well as redundant among the four FGFRs. The molecular mechanisms that would explain both specificity and redundant activities are not well understood. Two proximal substrates (FRS1 and FRS2) interact with the activated FGFR tyrosine kinases that are tyrosine-autophosphorylated. FRS1 is phospholipase Cγ, which binds to phosphorylated tyrosine 766 of FGFR1, and is phosphorylated by the kinase. Activation of FRS1 is not obligatory for the mitogenic activity of FGFR1 (3, 4). However, it is important for prostate epithelial cells to acquire a mitogenic response to FGFR1 and for other cellular activities stimulated by phospholipase Cγ (5).

FRS2 (also called SNT1, for suc1-associating nuclear target protein 1) is an adaptor protein that is anchored to the plasma membrane by virtue of myristoylation at the N terminus (6–8). FRS2 interacts with the intracellular juxtamembrane sequence of the FGFR through a conserved phosphotyrosine binding (PTB) domain adjacent to the C terminus of the myristoylation consensus sequence (9, 10). The PTB domain of FRS2 is homologous to and exhibits a similar three-dimensional structure as PTB domains of several other signaling adaptor proteins, including insulin receptor substrate 1. Phosphorylation of FRS2 in response to FGF treatment is associated with the FGF mitogenic signaling (6). The C-terminal half of FRS2 has multiple candidate phosphorylation sites as well as numerous signaling molecule binding sites, which include Grb2 that recruits upstream activators of the extracellular signal-regulated kinase 1/2 in the MAP kinase pathway. Therefore, FRS2 is considered an adaptor that connects FGFR to the MAP kinase pathway (5, 11–15). The fact that not all FGFR signaling is tightly associated with activation of the MAP kinase pathway (16, 17) prompted us to investigate alternative and potentially more direct means by which the FGFR transmits mitogenic signals.

The interaction of FRS2 with $p13^{suc1}$, a yeast cyclin-dependent kinase (Cdk)-binding protein important for cell cycle regulation (18), has been utilized together with anti-phosphotyrosine antibodies to precipitate and assess FGF-dependent phosphorylation of FRS2 for decades. Although a useful experimental tool, the interaction has not been associated with FGF signal transduction. Two mammalian homologues of Suc1, Cks1 and Cks2, have been identified (19–21). Cks1 is required for $p27^{Kip1}$ to interact with the Skp-2 (S-phase kinase-associated protein 2) ubiquitin ligase complex and promotes $p27^{Kip1}$ degradation (22–24). The degradation of $p27^{Kip1}$ in the late G_1 phase activates Cdk2-cyclin E and Cdk2-cyclin A complexes that, in turn, signal the cells to enter the S phase of the cell cycle (22, 23).

Despite the fact that Cks1 and Cks2 are homologues, the function of Cks2 is not clear. Cks2 has been implicated in the first metaphase/anaphase transition of mammalian meiosis (25). Mice lacking Cks2 are viable, but both sexes are sterile, in

¹ The abbreviations used are: FGF, fibroblast growth factor; FGFR, FGF receptor; FRS, FGF receptor substrate; GST, glutathione S-transferase; PTB, phosphotyrosine binding; MAP, mitogen-activated protein; Cdk, cyclin-dependent kinase; GFP, green fluorescent protein.

contrast to mice lacking Cks1 that are smaller than wild type (23). Cells derived from the Cks1 null mice proliferate at a reduced rate, consistent with elevated levels of p27^{Kip1} (23). Cellular levels of p27^{Kip1} are tightly controlled. The expression of p27^{Kip1} is frequently down-regulated in human tumors (26, 27), and the reduction correlates with a poor prognosis (28).

Although the interaction of Cks1 with p27^{Kip1} and Skp-2 triggers the G_1/S transition by inducing p27^{Kip1} ubiquitination and degradation, the potential upstream regulators of Cks1 have not been identified. Because of the homology of Suc1 to Cks1 and the historic interaction of Suc1 with the major FGFR kinase substrate FRS2, we asked whether the FGFR kinase might directly affect Cks1-mediated p27^{Kip1} degradation as a mechanism of FGFR induction of the G_1/S transition. Here we report that Cks1 associated with unphosphorylated FRS2 through the sequence encoding the PTB and myristoylation domains. Phosphorylation of FRS2 by the FGFR1 kinase in response to activating FGF ligands reduced the interaction and induced p27^{Kip1} degradation in mouse 3T3 cells. The release of Cks1 from FRS2 via activation of the FGFR kinase suggests a novel signaling pathway whereby a transmembrane receptor tyrosine kinase may directly activate the cell cycle through Cks1-mediated activation of cyclin-dependent kinases.

EXPERIMENTAL PROCEDURES
Construction and Expression of Recombinant Proteins

Construction of Cks-GST/GFP Fusion Proteins—Full-length cDNA for mouse Cks1 was amplified by reverse transcription-PCR from mouse embryo RNA pools with forward primer cks1a (CTCCTGCA-GAGCGATCATGTCGCACAAACA) and reverse primer cks1b (CTG-CAGGTACCTTTCTTTGGTTTC). Similarly, full-length cDNA for Cks2 was amplified by reverse transcription-PCR with forward primer cks2a (TTTCTGCAGCGCGCCGGCAGGATGGCCCAC) and reverse primer cks2b (TAAGGTACCTTTTTGTTGTTCTTT). The PCR products were cloned in pBluescript SK vector at PstI and KpnI restriction sites. After sequence verification, the PCR fragments of Cks1 and Cks2 were in-frame ligated to the 5'-end of the coding sequence for *Schistosoma japonicum* glutathione *S*-transferase (GST). The resulting cDNAs were subcloned into vector pVL1393 for preparation of recombinant baculo-viruses. Expression of Cks1- and Cks2-GST fusion proteins was evaluated with the anti-GST polyclonal antibody (29). The Cks cDNAs were also cloned into vector pEGFP-N3 for expression in mammalian cells as GFP-Cks fusion proteins that had a green fluorescence protein (GFP) tag at the N terminus or into vector pEGFP-C3 for expression as Cks-GFP fusion proteins that had a GFP tag at the C terminus.

Construction of FRS2 Mutants—The cDNA encoding the N terminus of ΔmFRS2-His that had a His tag at the C terminus was PCR-ampli-fied from the full-length FRS2 coding sequence with forward primer dm1 (CTGTTGCCCGGGTCCAGATAAAGACACTGT) and reverse primer dm2 (TCCACTAACTTGATCTCTTCCAAG). The cDNA coding for ΔpFRS2-His was PCR-amplified from the same template with forward primer ts1 (ACACCTGCCACCATGGGATTTGCTGCTCAGAAC) and reverse primer FRS2hisb (5). The cDNA coding for PTB-His was PCR-amplified with forward primer FRS2a (5) and reverse primer ptb2 (GTTCTGAGTACTAAATCCTGGAGT); the cDNA coding for ΔmPTB-His was PCR-amplified with forward primer dm1 and reverse primer ptb2. The cDNA fragments were ligated to C-terminal coding sequences of FRS2-His, and the resulting fragments were cloned in vector pBlue-script SK for sequence verification. Due to the lack of a translational initiation site, coding sequences for ΔmFRS2 and ΔmPTB were in-frame ligated to pCMV-Tag2 vector containing an artificial FLAG tag downstream of the translational initiation site. The molecular weights of the fusions were slightly higher than those of FRS2 and PTB, respec-tively, due to coding sequences of the vector. The cDNA fragments were then subcloned to vector pVL1393 for preparation of recombinant bacu-loviruses (29). Full-length FRS2-His fusion proteins were prepared as previously described (30).

Affinity Pull-down Assays

Pull-down with Glutathione Beads—sf9 cells (5 × 10^6) were infected with the indicated recombinant viruses for 3 days and lysed with 0.5% Triton X-100-phosphate-buffered saline. The cell lysates were mixed as indicated and incubated with glutathione beads (Amersham Bio-

sciences) or p13^{suc1}-GST beads (Upstate Biotechnology, Inc., Lake Placid, NY) at 4 °C for 2 h. The beads were washed with 0.1% Triton-phosphate-buffered saline four times, and specifically bound fractions were recovered with the SDS-sample buffer.

Pull-down with Nickel Beads—The cell lysates were mixed as indi-cated and diluted with equal volumes of the washing buffer (0.5 M NaCl, 0.1 M imidazole, and 10 mM Tris-HCl, pH 7.5). The mixtures were gently rocked with 30 μl of nickel-agarose beads (Amersham Biosciences) at 4 °C for 1 h. The FRS2-His-nickel-agarose complexes were then washed three times with the washing buffer, and specifically bound fractions were recovered from beads with the SDS-sample buffer.

Phosphorylation of FRS2 by FGFR1 Kinase—sf9 insect cells (5 × 10^6) were co-infected with the indicated FRS2- and FGFR1-bearing baculo-viruses for 3 days. The cells were incubated with 25 μg/ml heparin and 20 ng/ml FGF1 for 30 min at 27 °C where indicated and lysed as described above. The cell lysates were mixed and incubated with glu-tathione beads or nickel beads as indicated. Specifically bound fractions were divided into three aliquots, and electroblotted to nylon mem-branes. Tyrosine-phosphorylated FRS2 and FGFR1 were detected with anti-phosphotyrosine antibody 4G10 (Upstate Biotechnology). The total FRS2-His proteins were detected with anti-His tag antibody (Santa Cruz Biotechnology, Inc., Santa Cruz, CA), and total FGFR1 proteins were detected with anti-FGFR1 antibody 17A3 as indicated. The corre-sponding bands were visualized with ECL-plus chemiluminescent de-tection reagents (Amersham Biosciences).

Quantitation of Cellular p27^{Kip1} Proteins—The cells (2 × 10^5) in 6-well plates were brought to quiescence by incubation in medium containing 0.1% fetal bovine serum for 48 h. Then the cells were incu-bated with cycloheximide (2 mg/ml) for 1 h where indicated, followed by incubation with FGF2 (20 ng/ml) and heparin (2 μg/ml) for the indicated time. The cells were then lysed with 0.5% Triton-phosphate-buffered saline. Protein concentrations of the lysates were determined using the BCA protein assay reagent (Pierce). Aliquots equal to 5 μg of proteins were subjected to SDS-PAGE and then electroblotted to nylon mem-branes. Cellular levels of p27^{Kip1} were detected with anti-p27^{Kip1} anti-body (Santa Cruz Biotechnology). The corresponding bands were visu-alized with the ECL-plus chemiluminescent detection reagents.

RESULTS

FRS2-His Was Tyrosine-phosphorylated by the FGFR1 Ki-nase in sf9 Cells—To generate enough recombinant FRS2 pro-teins for biochemical studies, recombinant baculovirus bearing coding sequence for FRS2-His with a hexahistidine tag at the C terminus was generated. To determine whether FRS2-His was phosphorylated by the FGFR1 kinase, FRS2-His was co-ex-pressed with FGFR1 kinase in sf9 cells and pulled down with nickel-Sepharose beads. The bound fractions were subjected to Western blot with anti-phosphotyrosine and anti-His tag anti-bodies. Fig. 1A shows that FRS2-His was specifically tyrosine-phosphorylated by the FGFR1 kinase. Immunoblotting with anti-phosphotyrosine antibody revealed multiple bands with ap-parent molecular masses ranging from 55 to 85 kDa (Fig. 1A), which reflects differential phosphorylation of FRS2 (5, 31). To determine whether the phosphorylated FRS2-His exhibited the expected association with p13^{suc1}, the recombinant FRS2-His was incubated with p13^{suc1}-agarose beads, and the bound frac-tions were subjected to Western blotting with the indicated an-tibodies (30). Surprisingly, FRS2-His proteins were pulled down with the p13^{suc1}-GST beads independent of the presence of the FGFR1 kinase (Fig. 1B). This showed that the interaction of FRS2 and p13^{suc1} was tyrosine phosphorylation-independent.

Phosphorylation-dependent Association of FRS2 with Cks1— To determine whether the mammalian counterparts of yeast p13^{suc1} also associated with FRS2 and played roles in FGF signaling, mouse cDNAs coding for Cks1 and Cks2 were cloned and expressed with a GST tag at the N terminus to facilitate purification and identification (32). The Cks1-GST and Cks2-GST fusion proteins expressed in sf9 cells were soluble and bound to GSH-agarose beads (Fig. 2). In addition, Cks1-GFP and Cks2-GFP that had a GFP tag either at the N terminus or the C terminus were distributed in both cytosol and nucleus when overexpressed in NIH 3T3 cells (Supplemental Fig. 1).
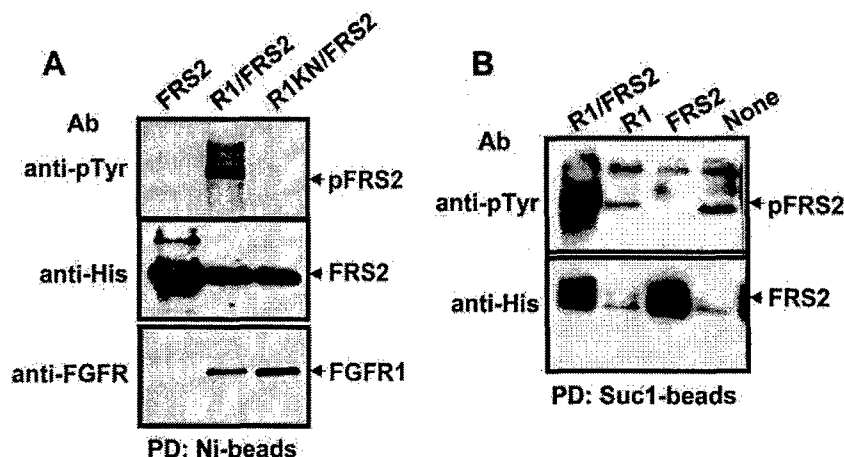
FIG. 1. *A*, specific phosphorylation of FRS2 by FGFR1 kinase. FRS2 from lysates of sf9 cells (equivalent to 5×10^5 cells) infected with baculoviruses bearing FRS2 and FGFR1 coding sequences as indicated were pulled down with nickel beads as described under "Experimental Procedures." The immobilized fractions were separated on SDS-PAGE, electroblotted to nylon membranes, and analyzed with the indicated antibodies (*top* and *middle panels*). *Bottom panel*, aliquots of the same lysates representing 1×10^6 cells were directly applied on SDS-PAGE, electroblotted to nylon membranes, and detected with anti-FGFR1 monoclonal antibody (32). *B*, phosphorylation-independent interaction of FRS2 with Suc1. sf9 cells (5×10^6) in T25 flasks were infected with the same baculoviruses, and the cells were lysed as described under "Experimental Procedures." The expressed FRS2 recombinant proteins (equivalent to 5×10^5 sf9 cells) were pulled down with Suc1-agarose beads as recommended by the manufacturer. After being washed with phosphate-buffered saline four times, the specifically bound fractions were eluted with SDS-sample buffer, and the eluants were divided into two aliquots. The samples were separated on SDS-PAGE, electroblotted to nylon membranes, and analyzed with the indicated antibodies. *Ab*, antibody; *anti-pTyr*, anti-phosphotyrosine monoclonal antibody; *anti-His*, anti-His tag polyclonal antibody; *pFRS2*, phosphorylated FRS2; *R1*, FGFR1; *R1KN*, kinase-inactive mutant of FGFR1 (5); *Ni*, nickel-agarose beads; *suc1*, GST-Suc1 agarose beads; *None*, uninfected sf9 cells; *PD*, pull-down.
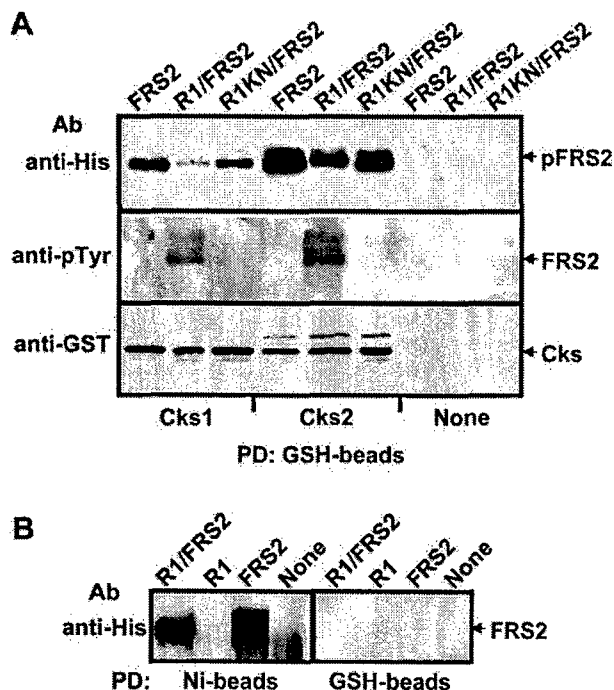

FIG. 2. *A*, phosphorylation-dependent interaction of FRS2 with Cks1. Cks1- and Cks2-GST expressed in 5×10^5 sf9 cells were immobilized on glutathione-agarose beads as described under "Experimental Procedures." The beads were then incubated with lysates of sf9 cells (equivalent to 5×10^5 cells) infected with baculoviruses bearing the indicated FGFR1 and FRS2 coding sequences. After being washed four times, specifically bound fractions were separated on SDS-PAGE, electroblotted to nylon membranes, and analyzed with the indicated antibodies as described under "Experimental Procedures." *B*, FRS2 did not bind to glutathione beads without Cks1-GST. The lysates equivalent to 5×10^5 sf9 cells infected with the same virus were incubated with nickel beads or GSH beads without Cks1- or Cks2-GST fusion proteins. After being washed four times, the bound fractions were analyzed by Western blot with the anti-His tag antibody. *Ab*, antibody; *anti-pTyr*, anti-phosphotyrosine antibody; *anti-His*, anti-His tag antibody; *anti-GST*, anti-GST antibody; *R1*, FGFR1; *R1KN*, kinase-inactive mutant of FGFR1; *pFRS2*, phosphorylated FRS2; *None*, uninfected sf9 cells; *PD*, pull-down.

This is similar to p13^{suc1} that gradually accumulates in the nucleus after it is microinjected into the cells (33).

To determine whether FRS2 associated with Cks1 and Cks2 and whether the association was tyrosine phosphorylation-dependent, sf9 cell-expressed FRS2 recombinant proteins, with and without coexpression with the FGFR1 kinase, were applied to GSH-agarose beads together with Cks1-GST or Cks2-GST. The bound fractions were divided into three aliquots and Western blotted with the indicated antibodies (Fig. 2A). Co-expression with the FGFR1 kinase abrogated the FRS2-Cks1 interaction, whereas it only reduced the FRS2-Cks2 interaction (Fig. 2A, *top panel*). Consistently, Western blot with anti-phosphotyrosine antibody revealed that more phosphorylated FRS2 was pulled down by Cks2 than by Cks1 (Fig. 2A, *middle panel*). Under similar conditions, FRS2 was not pulled down by GSH-agarose beads in the presence or absence of the FGFR1 kinase (Fig. 2B). This indicates that the pull-down occurs through interactions between FRS2 and Cks1-GST or Cks2-GST.

To confirm that the negative impact of FGFR1 kinase on FRS2-Cks1 interactions was due to activity of FGFR1 kinase and not due to competition between Cks1 and FGFR in interaction with FRS2, similar experiments were carried out with FRS2 coexpressed with a kinase-inactive mutant of FGFR1 (R1KN). The results showed that R1KN failed to phosphorylate FRS2 and also failed to abrogate the FRS2-Cks1 interaction (Fig. 2A). Together with the fact that the direct binding of FRS2 and FGFR1 is weak, since most of FRS2 cannot be pulled down by FGFR1, the data suggest that there is no competition between Cks and FGFR1 for interaction with FRS2. To determine whether the incubation with Cks1-GST or Cks2-GST caused FRS2 degradation, FRS2-His, with and without co-expression with FGFR1 kinase, was incubated with lysates of sf9 cells expressing Cks1-GST or Cks2-GST at 4 °C for 2 h. The FRS2-His in the mixtures was then pulled down with nickel-agarose beads, and the bound fractions were analyzed with the antibodies indicated in Fig. 3. The results showed that incubation with Cks1- and Cks2-GST did not induce FRS2 degradation. Together the results here suggest that unphosphorylated FRS2 associates with both Cks1 and Cks2 and that tyrosine phos-
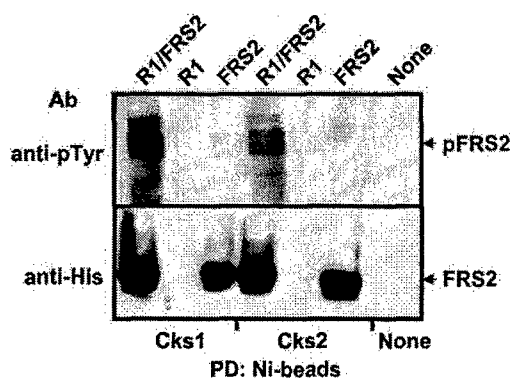
FIG. 3. **Incubation with Cks1 did not cause FRS2 degradation.** Lysates of sf9 cells (equivalent to 5×10^5 cells) infected with baculoviruses bearing FRS2 and FGFR1 coding sequences, as indicated, were mixed with lysates of sf9 cells (equivalent to 5×10^5 cells) infected with Cks1- or Cks2-GST. Uninfected sf9 cells were used as negative controls. The mixtures were incubated at 4 °C for 2 h, and the FRS2 proteins were then pulled down with nickel beads as described under "Experimental Procedures." After being washed four times, the specifically bound FRS2 was divided into two aliquots and analyzed by Western blot with the indicated antibodies. *Ab*, antibody; *anti-pTyr*, antiphosphotyrosine antibody; *anti-His*, anti-His tag antibody; *R1*, FGFR1; *pFRS2*, phosphorylated FRS2; *None*, uninfected sf9 cells; *PD*, pull-down.

phorylation of FRS2 by the FGFR1 kinase selectively causes release of Cks1 from FRS2, presumably as a consequence of interference of the FRS2-Cks1 interaction by tyrosine phosphorylation on FRS2.

Cks Associated with FRS2 via Conserved PTB and Myristoylation Domains—The N terminus of FRS2 has a short myristoylation consensus sequence followed by a conserved PTB domain that interacts with FGFR1 kinase and other receptor tyrosine. The C terminus has multiple candidate sites for tyrosine phosphorylation and interaction with downstream molecules. To identify FRS2 structural domains required for association with Cks1 and Cks2, a panel of FRS2 mutants was constructed for coexpression and interaction studies in sf9 cells. All of the mutants were hexahistidine-tagged at the C terminus (Fig. 4A) and, therefore, specifically bound to nickel-agarose beads (Fig. 4B). Affinity pull-down assays with GSH-agarose beads in the presence of Cks1- or Cks2-GST fusions showed that deletion of the sequence coding for PTB and myristoylation domain (ΔpFRS2) abolished the association of FRS2 with both Cks1 and Cks2. Deletion of the myristoylation sequence alone (ΔmFRS2) also significantly impaired the association (Fig. 4C). This suggests that conserved myristoylation and PTB domains of FRS2 are required for the interaction with Cks1 and Cks2. In all cases, the GSH-agarose beads alone failed to pull-down FRS2 and FRS2 constructs under the same conditions (Fig. 4C).

We then determined whether FRS2 associated with Cks1 and Cks2 directly through the PTB domain by construction of mutant PTB composed of solely the myristoylated N-terminal PTB domain and ΔmPTB without the myristoylation site (Fig. 4A). Pull-down assays showed that the PTB strongly interacted with both Cks1- and Cks2-GST independent of the FGFR1 kinase (Fig. 5A). Deletion of the N-terminal myristoylation sequence also significantly reduced the association with Cks1 and Cks2 (Fig. 5A). Separate results not shown here revealed that the FGFR1 kinase failed to phosphorylate the isolated PTB domain. Fig. 5B indicates that there was no interaction between FRS2 and GST and that the pull-down was specifically through the FRS2-Cks interaction.

FGF Induced p27^{Kip1} Degradation without New Protein Syntheses—Cks1 mediates degradation of p27^{Kip1}, a Cdk inhibitor,

through the ubiquitination pathway during the G_1/S transition of the cell cycle and promotes cell cycle progression (22, 23). To determine whether activation of the FGFR1 kinase induced degradation of p27^{Kip1} through releasing Cks1 from FRS2, NIH 3T3 cells expressing endogenous FGFR1 kinase (5) were synchronized by incubation in medium containing 0.1% serum for 48 h and then exposed to FGF2 for up to 48 h. The cellular levels of p27^{Kip1} protein were measured with anti-p27^{Kip1} antibodies (Fig. 6A). The results demonstrated that FGF2 significantly induced reduction of p27^{Kip1} at the protein level 6 h after the treatment. Cells constantly synthesize p27^{Kip1} during the cell cycle (27). Therefore, the tightly controlled oscillation of p27^{Kip1} is primarily achieved by post-translational regulation. To determine whether activation of the FGFR1 kinase accelerated p27^{Kip1} degradation instead of reducing new protein synthesis, quiescent 3T3 cells were treated with cycloheximide, a protein synthesis inhibitor, for 1 h before incubation with FGF2. Fig. 6B shows that p27^{Kip1} protein in the cycloheximide-treated cells was reduced 1 h after incubation with FGF2 and then decreased to below the detection limits 6 h after incubation with FGF2. This was significantly faster than that of the cells without exposure to FGF2 or cycloheximide. The results revealed that activation of the FGFR1 kinase accelerates degradation of p27^{Kip1}, and the degradation is independent of new protein synthesis. This suggests that degradation of p27^{Kip1} is a result of cascade reactions in the existing signaling networks (Fig. 7) rather than a result of changes at the gene expression level.

DISCUSSION

The interaction between p13^{suc1} and FRS2 has been utilized as an experimental tool to assess FGFR-induced phosphorylation of FRS2 for decades. However, the interaction has largely been assumed to be fortuitous and not of functional significance in FGF signaling. Here we report that Cks1, a mammalian homologue of p13^{suc1}, associated with the non-tyrosine-phosphorylated FRS2. Activation of the FGFR1 tyrosine kinase led to tyrosine phosphorylation of FRS2, released Cks1 from FRS2, and promoted p27^{Kip1} degradation. In addition, FRS2 bound to Cks1 via the conserved N-terminal sequence consisting of the PTB and myristoylation domains; deletion of the sequence abrogated the association. Deletion of the myristoylation domain alone also impaired the interaction. The FRS2 myristoylation site is composed of 6 amino acid residues (MGSCCS) located at the N terminus, which affixes FRS2 to the plasma membrane when it is myristoylated. It is likely that myristoylation and the membrane anchorage of FRS2 are important for the three-dimensional structure of the PTB domain to interact with Cks1 and Cks2, although the possibility that the myristoylation domain is a part of the Cks binding site cannot be ruled out.

FRS2 utilizes different sets of amino acid residues for interacting with Trk and other receptor tyrosine kinases (9, 10). Currently, it is unknown how the PTB domain interacts with Cks1, although the data here suggest that the sequence downstream of the PTB domain inhibits the interaction when it is phosphorylated by FGFR1 kinase. Unlike Cks1 that only bound to unphosphorylated FRS2, Cks2 also bound to phosphorylated FRS2. The functional significance of the interaction remains to be determined.

p27^{Kip1} belongs to the Cip/Kip family that negatively regulates Cdk kinase activity and plays a pivotal role in regulating mitogenic responses of cells to extracellular signals. The mRNA level of p27^{Kip1} is fairly constant during cell cycles, and the cellular level of p27^{Kip1} proteins is regulated primarily at the posttranslational level through ubiquitination-mediated proteolysis. Cks1 is required for association of p27^{Kip1} to the SCF ubiquitin ligase complex consisting of S-phase-associated protein 2 (Skp2), Cul-1, and ROC1/Rbx1. The results here show
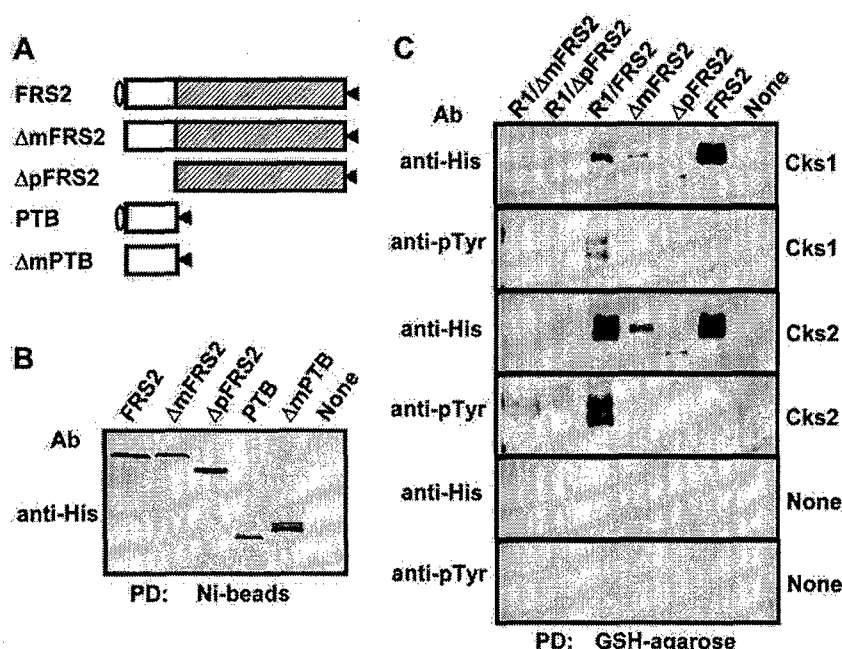
Cks1 in FGFR Mitogenic Signaling

FIG. 4. **Structural domains of FRS2 required for association with the Cks.** *A*, schematic of FRS2 mutants. *Oval*, the conserved myristoylation sequence; *open box*, the PTB domain; *hatched box*, the C-terminal sequence; *triangle*, the hexahistidine tag. *B*, expression of FRS2 mutants. The FRS2 proteins from 5×10^5 sf9 cells were pulled down with nickel-agarose beads, and the bound fractions were separated on SDS-PAGE, electroblotted to nylon membranes, and detected with anti-His polyclonal antibody. Note that the molecular weights of ΔmFRS2 and ΔmPTB were slightly higher than those of FRS2 and PTB, respectively, due to vector coding sequences as described under "Experimental Procedures." *C*, association of FRS2 with Cks required the PTB domain. Cks1- and Cks2-GST expressed in 5×10^5 sf9 cells were immobilized on glutathione-agarose beads as described under "Experimental Procedures". The beads were then incubated with lysates of sf9 cells (equivalent to 5×10^5 cells) infected with baculoviruses bearing coding sequences for the indicated FRS2 mutants and FGFR1. After being washed four times, bound fractions were analyzed by Western blot with the indicated antibodies. *Ab*, antibody; *anti-pTyr*, anti-phosphotyrosine antibody; *anti-His*, anti-His tag antibody; *R1*, FGFR1; *None*, uninfected sf9 cell lysates; *PD*, pull-down.
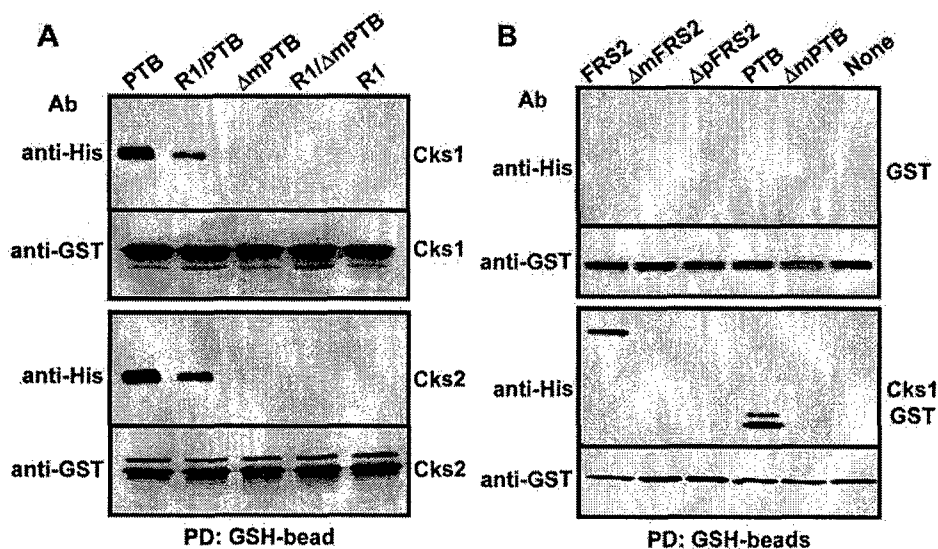

FIG. 5. *A*, interaction of the PTB domain with Cks1 and Cks2. Cks1- and Cks2-GST expressed in 5×10^5 sf9 cells were immobilized on glutathione-agarose beads as described in the legend to Fig. 2. The beads were then incubated with lysates of sf9 cells (equivalent to 5×10^5 cells) infected with baculoviruses bearing coding sequences for the indicated PTB constructs and FGFR1. After being washed four times, bound fractions were Western blotted with the anti-His tag antibody. The same membranes were stripped off bound antibodies, according to manufacturer's instructions, and reprobed with anti-GST antibody. *B*, FRS2 did not bind to GST. Cks1-GST fusion proteins or GST alone expressed in 5×10^5 sf9 cells was immobilized on glutathione-agarose beads as described in *A*. The beads were then incubated with lysates of sf9 cells (equivalent to 5×10^5 cells) infected with baculoviruses bearing coding sequences for the indicated FRS2 constructs. The bound fractions were Western blotted with anti-His tag antibody. The same membranes were stripped off of antibodies and reprobed with anti-GST antibody as in *A*. *Ab*, antibody; *anti-GST*, anti-GST antibody; *anti-His*, anti-His tag antibody; *R1*, FGFR1; *None*, uninfected sf9 cell lysates; *PD*, pull-down.

that unphosphorylated FRS2 bound to Cks1; the FGFR phosphorylates FRS2 upon stimulation by the FGF and releases Cks1 from FRS2. Thereafter, the freed Cks1 may induce degradation of p27[Kip1] and signal the cells entering mitosis by activating Cdk-cyclin A/E complexes (22, 23). The results firstly suggest that the FGFR1 tyrosine kinase may transmit mito-

genic signals to downstream cascades directly through regulating Cdk-cyclin complexes, as illustrated in Fig. 7.

Expression of p27[Kip1] is frequently down-regulated at the protein and mRNA levels in tumor cells (28), and the decrease is significantly correlated with malignancy of tumors (35, 36). It has been proposed that p27[Kip1] acts as a rheostat rather than
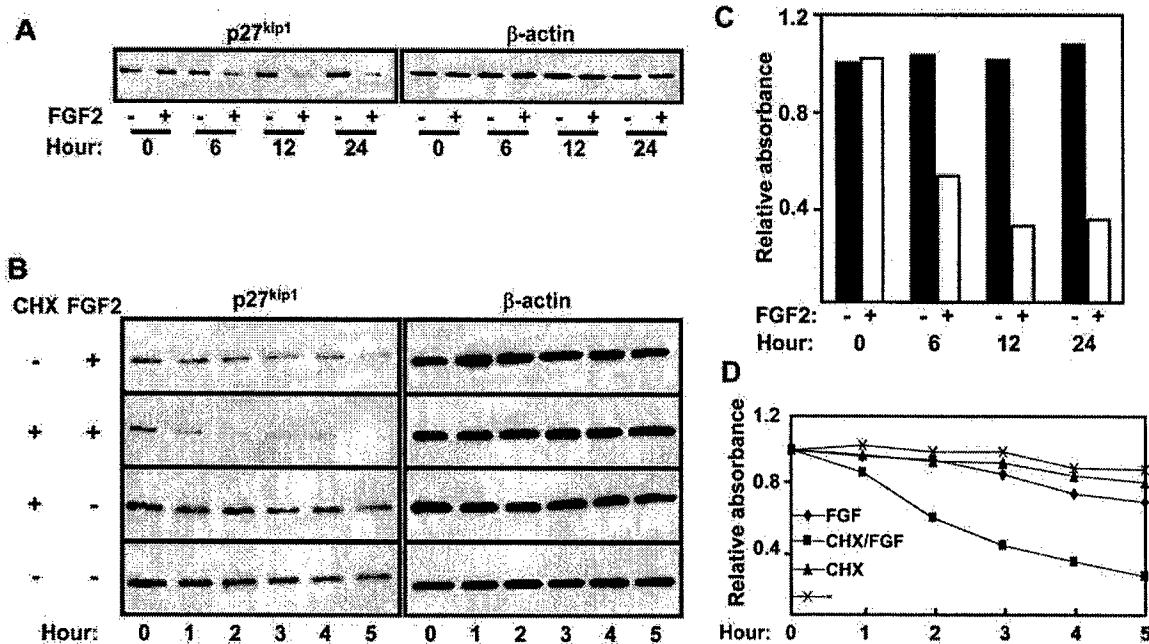
FIG. 6. FGF mediated degradation of p27^{Kip1} without new protein synthesis. *A*, mouse 3T3 cells (2 × 10^5) in 6-well plates were cultured in medium with 0.1% fetal bovine serum for 48 h and then treated with FGF2, where indicated, for the indicated hours before being lysed with the lysis buffer. Aliquots of the lysates (equivalent to 5 μg of protein) were loaded onto each lane. After being electroblotted to nylon membrane, p27^{Kip1} was detected with the anti-p27^{Kip1} antibody as described under "Experimental Procedures." After exposure, the same membrane was stripped off of the bound antibodies, as suggested by the manufacturer, and reprobed with anti-β-actin antibody for loading controls. *B*, The 3T3 cells brought to quiescence similarly as in A were treated with cycloheximide (2 mg/ml) for 1 h, where indicated, before incubation with FGF2. The cells were lysed at the indicated hours after FGF2 treatments and analyzed by Western blot as above. *C* and *D*, the specific bands representing p27^{Kip1} in *A* and *B*, respectively, were scanned with a densitometer. The integrated absorbance of each band was normalized to that of the band representing β-actin at each time point, and the ratios of normalized absorbance of samples to that of control samples (without FGF2 treatment) were plotted. *CHX*, cycloheximide.
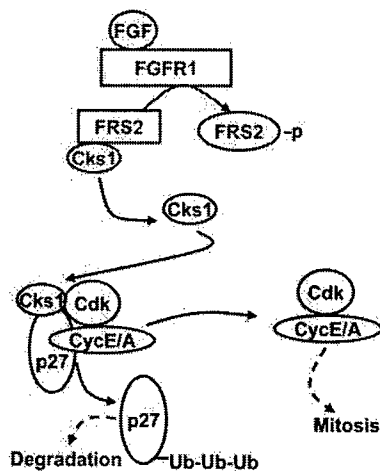

FIG. 7. Schematic of the direct regulation of Cdk by the FGFR1 mitogenic signaling pathway. Phosphorylation of FRS2 by the FGFR1 kinase releases Cks1. The freed Cks1 associates with the p27^{Kip1}-Cdk-cyclin complex, induces the formation of the p27^{Kip1}-SCF ubiquitin ligase complex, triggers degradation of p27^{Kip1}, and signals cells to undergo the G$_1$/S transition by releasing and activating the Cdk-cyclin A/E complexes. *CycE/A*, cyclin E or cyclin A; *Ub*, ubiquitin.

as an on-off switch to control growth and neoplasia, since tumor suppression by p27^{Kip1} is critically dependent on the absolute level of p27^{Kip1} protein within cells (28). Unlike epithelial cells from benign prostate tumors and normal prostate that express the FGFR2 isoform, malignant prostate cells often express the nonresident FGFR1 isoform (1, 5, 37–39). Ectopic appearance of constitutively active FGFR1 kinase in prostate epithelial cells induces prostate hyperplasia and high grade prostatic intraepithelial neoplasia in transgenic mice (40, 41). Therefore, chronic FGFR1-mediated p27^{Kip1} degradation may play a role in perturbation of prostate tissue homeostasis and tumor pro-

motion. Sequestration of Cks1 by FRS2 and its control by FGFR1 kinase may be of therapeutic value in cancer prevention and treatment.

The kinase domains of the four FGFRs share a high similarity in amino acid sequence and elicit similar and redundant regulatory activities in some experimental systems (1). In other experimental systems, the FGFRs elicit individual isotype-specific and sometimes even opposite regulatory activities (2). The resident FGFR2 kinase in bladder (42), prostate (38, 39), and salivary tumor epithelial cells (34) promotes homeostasis and suppresses the tumor phenotype. This is in contrast to the ectopic FGFR1 that appears in malignant tumors and promotes proliferation and tumorigenesis (1, 2, 5, 38). The resident FGFR2 and ectopic FGFR1 differently phosphorylate FRS2 and activation of the MAP kinase pathway in prostate epithelial cells (2, 30). Currently, we do not know whether the FGFR2 also mediates release of Cks1 from FRS2 or whether activation of the MAP kinase pathway affects release of Cks1 from tyrosine-phosphorylated FRS2 or *vice versa* in prostate epithelial cells.

In summary, here we report that the release of Cks1 from tyrosine-phosphorylated FRS2 possibly mediates mitogenic signals of the FGFR1 kinase. Determination of whether the four FGFR kinases differ in releasing Cks1 from FRS2 by phosphorylation and whether the release is regulated by other signaling pathways will shed light on understanding the mechanism underpinning the FGF signaling pathway.

REFERENCES

1. McKeehan, W. L., Wang, F., and Kan, M. (1998) *Prog. Nucleic Acids Res. Mol. Biol.* **59**, 135–176
2. Wang, F., and McKeehan, W. L. (2003) *Handbook of Cell Signaling*, Vol. 1 (Bradshaw, R., and Dennis, E., eds) pp. 265–270, Academic/Elsevier Press, New York

3. Mohammadi, M., Dionne, C. A., Li, W., Li, N., Spivak, T., Honegger, A. M., Jaye, M., and Schlessinger, J. (1992) *Nature* **358,** 681–684
4. Peters, K. G., Marie, J., Wilson, E., Ives, H. E., Escobedo, J., Del Rosario, M., Mirda, D., and Williams, L. T. (1992) *Nature* **358,** 678–681
5. Wang, F., McKeehan, K., Yu, C., and McKeehan, W. L. (2002) *Cancer Res.* **62,** 1898–1903
6. Kouhara, H., Hadari, Y. R., Spivak-Kroizman, T., Schilling, J., Bar-Sagi, D., Lax, I., and Schlessinger, J. (1997) *Cell* **89,** 693–702
7. Xu, H., Lee, K. W., and Goldfarb, M. (1998) *J. Biol. Chem.* **273,** 17987–17990
8. Lin, H. Y., Xu, J., Ischenko, I., Ornitz, D. M., Halegoua, S., and Hayman, M. J. (1998) *Mol. Cell. Biol.* **18,** 3762–3770
9. Dhalluin, C., Yan, S. K., Plotnikova, O., Lee, W. K., Zeng, L., Kuti, M., Mujtaba, S., Goldfarb, P. M., and Zhou, M. M. (2000) *Mol. Cell* **6,** 921–929
10. Yan, K. S., Kuti, M., Yan, S., Mujtaba, S., Farooq, A., Goldfarb, M. P., and Zhou, M. M. (2002) *J. Biol. Chem.* **277,** 17088–17094
11. Lopez, M. E., and Korc, M. (2000) *J. Biol. Chem.* **275,** 15933–15939
12. Ong, S. H., Guy, G. R., Hadari, Y. R., Laks, S., Gotoh, N., Schlessinger, J., and Lax, I. (2000) *Mol. Cell. Biol.* **20,** 979–989
13. Hadari, Y. R., Gotoh, N., Kouhara, H., Lax, I., and Schlessinger, J. (2001) *Proc. Natl. Acad. Sci. U. S. A.* **98,** 8578–8583
14. Melillo, R. M., Santoro, M., Ong, S. H., Billaud, M., Fusco, A., Hadari, Y. R., Schlessinger, J., and Lax, I. (2001) *Mol. Cell. Biol.* **21,** 4177–4187
15. Xu, H., and Goldfarb, M. (2001) *J. Biol. Chem.* **276,** 13049–13056
16. Ribisi, S., Jr., Mariani, F. V., Aamar, E., Lamb, T. M., Frank, D., and Harland, R. M. (2000) *Dev. Biol.* **227,** 183–196
17. Corson, L. B., Yamanaka, Y., Lai, K. M., and Rossant, J. (2003) *Development* **130,** 4527–4537
18. Brizuela, L., Draetta, G., and Beach, D. (1987) *EMBO J.* **6,** 3507–3514
19. Hadwiger, J. A., Wittenberg, C., Mendenhall, M. D., and Reed, S. I. (1989) *Mol. Cell. Biol.* **9,** 2034–2041
20. Richardson, H. E., Stueland, C. S., Thomas, J., Russell, P., and Reed, S. I. (1990) *Genes Dev.* **4,** 1332–1344
21. Patra, D., and Dunphy, W. G. (1998) *Genes Dev.* **12,** 2549–2559
22. Ganoth, D., Bornstein, G., Ko, T. K., Larsen, B., Tyers, M., Pagano, M., and Hershko, A. (2001) *Nat. Cell Biol.* **3,** 321–324
23. Spruck, C., Strohmaier, H., Watson, M., Smith, A. P., Ryan, A., Krek, T. W., and Reed, S. I. (2001) *Mol. Cell* **7,** 639–650
24. Seeliger, M. A., Breward, S. E., Friedler, A., Schon, O., and Itzhaki, L. S. (2003) *Nat. Struct. Biol.* **10,** 718–724
25. Spruck, C. H., de Miguel, M. P., Smith, A. P., Ryan, A., Stein, P., Schultz, R. M., Lincoln, A. J., Donovan, P. J., and Reed, S. I. (2003) *Science* **300,** 647–650
26. Cordon-Cardo, C., Koff, A., Drobnjak, M., Capodieci, P., Osman, I., Millard, S. S., Gaudin, P. B., Fazzari, M., Zhang, Z. F., Massague, J., and Scher, H. I. (1998) *J. Natl. Cancer Inst.* **90,** 1284–1291
27. Sgambato, A., Cittadini, A., Faraglia, B., and Weinstein, I. B. (2000) *J. Cell. Physiol.* **183,** 18–27
28. Philipp-Staheli, J., Payne, S. R., and Kemp, C. J. (2001) *Exp. Cell Res.* **264,** 148–168
29. Wang, F., Lu, W., McKeehan, K., Mohamedali, K., Gabriel, J. L., Kan, M., and McKeehan, W. L. (1999) *Biochemistry* **38,** 160–171
30. Wang, F. (2002) *In Vitro Cell Dev. Biol. Anim.* **38,** 178–183
31. Ong, S. H., Goh, K. C., Lim, Y. P., Low, B. C., Klint, P., Claesson-Welsh, L., Cao, X., Tan, Y. H., and Guy, G. R. (1996) *Biochem. Biophys. Res. Commun.* **225,** 1021–1026
32. Wang, F., Kan, M., McKeehan, K., Jang, J. H., Feng, S., and McKeehan, W. L. (1997) *J. Biol. Chem.* **272,** 23887–23895
33. Hepler, P. K., Sek, F. J., and John, P. C. (1994) *Proc. Natl. Acad. Sci. U. S. A.* **91,** 2176–2180
34. Zhang, Y., Wang, H., Toratani, S., Sato, J. D., Kan, M., McKeehan, W. L., and Okamoto, T. (2001) *Proc. Natl. Acad. Sci. U. S. A.* **98,** 11336–11340
35. Macri, E., and Loda, M. (1998) *Cancer Metastasis Rev.* **17,** 337–344
36. Fernandez, P. L., Hernandez, L., Farre, X., Campo, E., and Cardesa, A. (2002) *Pathobiology* **70,** 1–10
37. Yan, G., Wang, F., Fukabori, Y., Sussman, D., Hou, J., and McKeehan, W. L. (1992) *Biochem. Biophys. Res. Commun.* **183,** 423–430
38. Feng, S., Wang, F., Matsubara, A., Kan, M., and McKeehan, W. L. (1997) *Cancer Res.* **57,** 5369–5378
39. Matsubara, A., Kan, M., Feng, S., and McKeehan, W. L. (1998) *Cancer Res.* **58,** 1509–1514
40. Jin, C., McKeehan, K., Guo, W., Jauma, S., Ittmann, M. M., Foster, B., Greenberg, N. M., McKeehan, W. L., and Wang, F. (2003) *Cancer Res.* **63,** 8784–8790
41. Wang, F., McKeehan, K., Yu, C., Ittmann, M., and McKeehan, W. L. (2004) *Prostate* **58,** 1–12
42. Ricol, D., Cappellen, D., El Marjou, A., Gil-Diez-de-Medina, S., Girault, J. M., Yoshida, T., Ferry, G., Tucker, G., Poupon, M. F., Chopin, D., Thiery, J. P., and Radvanyi, F. (1999) *Oncogene* **18,** 7234–7243